

Short Communication

## Corrosion Behaviour of Various Superheater Steels in Cleaning Solutions

Xigang Yang<sup>1</sup>, Hao Zhang<sup>2</sup>, Yu Tan<sup>2,\*</sup>

<sup>1</sup> Guodian Science and Technology Research Institute Limited, Nanjing, Jiangsu, China

<sup>2</sup> Department of Environment Science and Engineering, North China Electric Power University, Baoding, Hebei, China

\*E-mail: [lucifertan@163.com](mailto:lucifertan@163.com)

Received: 19 March 2020 / Accepted: 15 July 2020 / Published: 10 August 2020

---

In recent years, with the increase in the national power supply demand, a large number super-critical units have been put into production in thermal power plants. The high-parameter units of thermal power plants have generally participated in peak shaving, and the working conditions have changed greatly. The over-temperatures, squibs and turbine blade rushes caused by superheater scales are becoming increasingly serious and widespread. Adapting superheater oxide skin chemical cleaning technology to new production conditions is an effective way to solve this problem. In this paper, the corrosion behaviour of various steels used for boiler superheaters in aqueous chemical cleaning is investigated.

---

**Keywords:** Corrosion behaviour; chemical cleaning; weight-loss method; steel

### 1. INTRODUCTION

A superheater in a thermal power plant is a heated surface in a boiler that further heats steam from a saturated temperature to a superheated temperature. It consists of a number of parallel tubes and inlet and outlet headers that are usually made of seamless alloy, which can improve the thermal efficiency and overall power output. The temperature of the medium in the high-temperature superheater tube is the highest, and it is arranged in the area where the temperature of the flue gas is high. Due to the high temperature, pressure, service time and aggressive environment, the superheater tube may suddenly rupture, and the initiation mechanism may be caused by creep, oxidation, overheating, stress cracking, thermal fatigue, ash and erosion[1].

Since the water (steam) circulating in the superheater exhibits oxidizing properties at a high temperature, the superheater reacts with the residual oxygen in the steam to form scale in the high-temperature flue gas environment. In particular, the frequent start-stop process or steam temperature fluctuation caused by the deep peaking of the thermal power plant causes the service temperature of the superheater to fluctuate repeatedly around 570°C, so the iron oxide generated in the furnace tube is not

only one phase. Since the expansion coefficients of the phases are different from those of the metal matrix, they are detached from the superheater tubes during the start-stop process. After the oxidized product falls off, it partially enters the steam turbine with superheated steam, causing erosion of the blade, which in turn causes problems such as turbine shake or shaft vibration[2]. Part of it may deposit in the superheater tubes, causing clogging of the superheater tubes or slowing of the cooling medium, which in turn causes local overheating of the superheaters. Excessive temperatures caused by overheating or long-term high-temperature creep in a short period of time can cause the metal material service life to be shorter than the design life. Usually, short-term overheating of the tube causes severe local deformation and expansion due to actual failure. The material is thinned due to high-temperature softening, and there is usually a bell-shaped break at the crack. Another feature that is easily overlooked is the increase in the hardness of the metal material near the opening during shutdown inspections, usually due to the similar ‘quenching’ of the metal by steam during breakage. Superheater bursting inevitably leads to unplanned downtime of the power plant, which has a major impact on the safety of the power plant. Generally, the problem of superheater squibs mainly occurs through the ‘replacement’ and ‘blowpipe’ methods[3-6]. Although the former can fundamentally solve the problem of superheater squibs, the cost is extremely high. The effect of the latter is not satisfactory because the superheated steam cannot totally remove the scale totally, and high-pressure gas purge in the cold state does not address the problem of a scale that does not easily come fall off.

In general, we recommend solving this problem of excessive iron oxide generation in the superheater by chemical cleaning. With the proper mixing of the chemical cleaning reagents, the amount of peeling of the scale is small, the dissolution effect is good, and the corrosion rate of the material is low. The austenitic stainless-steel material has no special requirements for superheater cleaning, such as intergranular corrosion, to ensure the cleaning quality. It is still necessary to determine the effectiveness of superheater tube cleaning by means of topography, including visual observation, optical microscopy, electron microscopy, XRD scale analysis, etc. The specific indicators should be determined according to the actual working conditions[7-8].

To control costs, thermal power plants usually use inorganic acid to clean carbon steel and low-alloy steel power station boiler bodies, but for alloy steel superheater tubes, organic acids such as EDTA, citric acid (ammonia) glycolic acid, and diethyl ether should be used[9]. Citric acid and EDTA have good removal effects on conventional iron scales, but due to the complex composition of the scale samples in the operation unit, especially when there are corrosion pits in the heated surface of the pipe, the scale in the pits cannot be completely removed by these reagent. Their removal ability is weak. Citric acid easily produces iron citrate precipitation during the cleaning process, which affects the quality of chemical cleaning. For industrial grade organic acids, the halogen ion content should be checked prior to use. In this experiment, the effects of different acids and their compounding processes on the corrosion behaviour of boiler superheater steel were studied on a simulated platform. Corresponding research was carried out on the sensitivity of intergranular corrosion[10].

## 2. EXPERIMENTAL METHODS

### 2.1 Weight loss testing

In this experiment, austenitic 304 stainless steel was the main focus. Additionally, the alloy structural steel 12CrMoV, martensitic heat resistant steel T91, and super austenitic stainless steel TP310 were employed in this experiment. Their components are listed in Table 1. All the alloy materials were cut into 2×10×50 mm pieces and mechanically polished with SiC papers. Then, the specimens were first cleaned in distilled water and then in ethanol by an ultrasonic machine and kept in a dry box. Four typical kinds of cleaning processes, including citric acid, glycolic acid and formic acid mixed solution, glycolic acid and citric acid mixed solution, and EDTA, were employed in this experiment, which are listed in Table 2. It should be highlighted that all the electrolytes were supplemented with the proper corresponding corrosion inhibitors and additives.

**Table 1.** Material compositions.

	Element wt%												
	Fe	Cr	Ni	Mn	Mo	Cu	Si	N	C	P	S	V	Nb
SS304	Ba.	18.14	8.07	1.64	0.46	0.51	0.58	0.07	0.024	0.034	0.001	-	-
TP310	Ba.	25.52	19.73	1.45	-	-	0.67	-	0.035	0.033	0.028	-	-
12CrMoV	Ba.	1.07	0.02	-	0.28	0.021	-	-	0.12	0.022	0.18	0.19	-
T91	Ba.	8.49	0.37	0.49	0.93	-	0.38	0.045	0.11	0.004	0.009	0.211	0.087

**Table 2.** Chemical cleaning electrolyte compositions and cleaning processes.

	Content(s) (wt)	pH	Corrosion inhibitor concentration (wt)	Temperature (°C)	Time (h)
Citric acid	5%	3.8	0.4%	95	8
Glycolic acid and Formic acid	Glycolic acid 2% + Formic acid 1%		0.4%	95	8
Glycolic acid and Citric acid	Glycolic acid 2% + Citric acid 1%		0.4%	95	8
EDTA	5%	9.0	0.4%	130	8

To simulate the actual cleaning conditions, a static autoclave was built, as shown in Fig. 1, and nitrogen gas was added to promote mass transfer during cleaning. Each group of specimens was placed in an autoclave and immersed in the corresponding solutions for 8 h of oxidation at 95°C. After removal from the autoclave, all the specimens were cleaned in acetone by an ultrasonic machine and were ready

for surface investigations. Before and after being placed in the autoclave, each specimen was measured according to the weight-loss method.

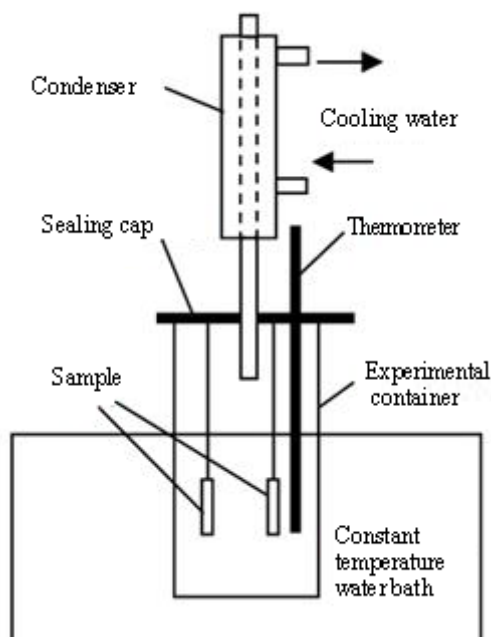


**Figure 1.** Schematic diagram of the autoclave for the weight-loss test.

### 2.2 Study on the sensitivity of the intergranular corrosion of austenitic steel

In the cleaning of the superheater tube in the boiler, the stress corrosion sensitivity of austenitic steel during or after cleaning is a key issue that should be noted. Generally, this sensitivity is determined by the properties of the austenitic steel; its grain boundaries are not resistant to  $\text{Cl}^-$ . If the stress corrosion of steel for boiler tubes is caused by chemical cleaning, it is worth considering whether it should be cleaned. For a deeper understanding, the SS304 specimen was employed to evaluate the sensitivity of the intergranular corrosion of austenitic steel in this research. A mixed solution of glycolic acid and formic acid was used as the cleaning solution. Additionally,  $\text{Fe}^{3+}$  was added to enhance the solution oxidative capacity. The test method was the same as above. The difference was that the experimental time was extended to 48 h. A metallographic microscope was used to observe the intergranular corrosion on the surface.

### 2.3 Study on the stress corrosion sensitivity of austenitic stainless steel

According to the requirements for processing the C ring in GB/T15970.5-1998, the 304 tube was cut into an outer diameter of 34 mm, a wall thickness of 2 mm and a width of 20 mm and aligned with the C-ring of 60 degrees. The stress corrosion test adopts a constant displacement loading method for the C-ring; bolts were tightened along the centre of the ring diameter, where an ultimate stress was applied. Then, the samples were cleaned with distilled water, cleaned with ethanol and stored in a dry box.

The cleaning solution was mixed with 2% glycolic acid and 1% formic acid, and the sample was immersed in a static autoclave and oxidized at 95°C for 120 h. Then, the samples were removed from the autoclave, rinsed with distilled water, and subjected to surface inspection with a metallographic microscope.

#### 2.4 Study on the Electrochemical Behaviour of Superheater Steels

Additionally, to better understand the corrosion behaviour, potentiodynamic polarization was employed to evaluate the corrosion rates of 304 stainless steel and TP310 stainless steel in various chemical cleaning solutions. A three-electrode system was established to test the potentiodynamic polarization. The samples were the working electrode. The Pt electrode worked as the counter electrode, and a saturated calomel electrode (SCE) was used as the reference electrode. A Parstat2273 electrochemical workstation controlled by a computer was employed to carry out electrochemistry tests with a scan rate of 1 mV/s[11].

### 3. RESULTS

#### 3.1 Weight loss testing

In this test, a hanging weight loss method was adopted. Five parallel samples were tested in each group. The corrosion rate formula was used to calculate the corrosion rate of each material sample in different environments, and the weight loss data were in line with the national standards. As shown in Fig. 2, the corrosion rate data obtained in the figure were obtained by averaging 5 data points from each test.

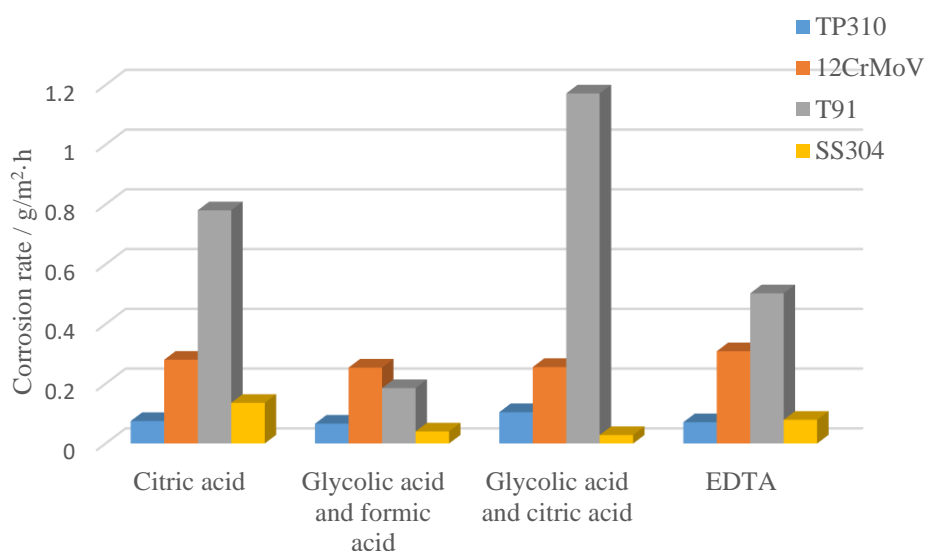


**Figure 2.** Corrosion rates of various steels in different chemical cleaning electrolytes.

Different steel types exhibited different weight loss behaviours in different chemical cleaning solutions. A typical trend was that the two austenitic alloy steels exhibited low deterioration indicators in the cleaning solutions, that is, their corrosion rates were low. For 12CrMoV, the corrosion rates in different chemical cleaning solutions were similar. T91 exhibited significantly high corrosion rates in solutions containing citric acid. For the 304 austenitic stainless steel of main concern, the corrosion rate in solution containing glycolic acid was significantly lower than that in solution containing citric acid, indicating that the homogeneous corrosion resistance of the austenitic stainless steel was not strong. It should be emphasized that, as works at higher cleaning temperature in the EDTA cleaning solution, for each material sample, the corrosion rates were generally considered not too high in this solution. Generally, the measured corrosion rates were much lower than the rates specified in the Guidelines for Chemical Cleaning of Boilers in Thermal Power Plants (DL/T 794-2001).

### 3.2 Electrochemical testing

From the above weight-loss tests, it was concluded that the samples of SS304 and TP310 had good corrosion resistance. To better understand the corrosion behaviour of SS304 and TP310 in cleaning solution, an electrochemical test was employed to test the potentiodynamic polarization. The experiment used a three-electrode system, namely, a saturated calomel electrode (SCE) as a reference electrode, a platinum electrode as an auxiliary electrode, and a sample as a working electrode. The electrochemical workstation used Parstat2273, which connected the three-electrode system to the electrochemical workstation. The experiment was carried out in a 95°C water bath. After the open circuit potential was basically stable, dynamic potential polarization curve scanning was started. The scanning range of the dynamic potential polarization scanning potential was 0.2 V on both sides of the open circuit potential, and the scanning rate was 1 mV/s. The potentiodynamic polarization curves of SS304 and TP310 in the glycolic acid and formic acid compound solution at 95°C are shown in Fig. 3.

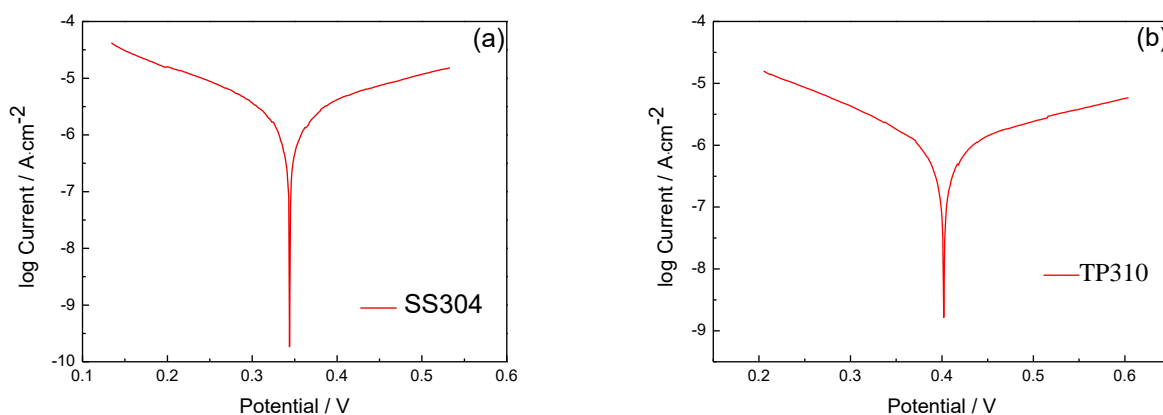


**Figure 3.** (a) Polarization curve of SS304 in glycolic acid and formic acid solution in a 95°C water bath; (b) Polarization curve of TP310 in glycolic acid and formic acid solution in a 95°C water bath.

The corrosion current density value of SS304 in glycolic acid and formic acid solution was  $5.5522 \text{ A}\cdot\text{cm}^{-2}$ , and the corrosion current density value of TP310 in glycolic acid and formic acid solution was  $6.0125 \text{ A}\cdot\text{cm}^{-2}$ . It could be seen that the corrosion current density values of SS304 and TP310 in the cleaning solution were relatively low, indicating that their corrosion resistances in the cleaning solution were relatively strong. There were no obvious passivation areas in the cleaning solution. Comparing these two materials, the corrosion current density of SS304 in the cleaning solution was slightly higher than that of TP310, indicating that the corrosion resistance of TP310 stainless steel in the cleaning solution was stronger than that of SS304.

### *3.3 Intergranular corrosion and stress corrosion testing*

Among domestic and foreign power generation companies, austenitic stainless steel is widely used in superheater materials because of its good corrosion resistance. However, chemical cleaning may corrode superheater tubes [12]. Therefore, we selected 4 kinds of typical materials, as well as four typical cleaning processes, and studied the corrosion of the superheater during the cleaning process, and the weight loss data met the national standards. However, the unilateral weight-loss data did not sufficiently explain the problem. Austenitic steel is subject to two major types of harmful corrosion, namely, intergranular corrosion and stress corrosion. Intergranular corrosion greatly bonds to the metal grains and reduces the strength of the material. In severe cases, it may cause the material to rupture and damage the equipment, which reduces the service life of the tube, and may even cause accidents and unpredictable losses in a power plant[13-16]. The superheaters in power station boilers are mainly made of austenitic stainless steel and connected by welding. During the welding process, unavoidable residual stress occurs near the welding zone, and stress occurs when the pipe is bent or dislocated. In a certain corrosive medium, stress corrosion cracking occurs in austenitic stainless steel[17]. We are concerned that these two types of corrosion might occur during chemical cleaning, and thus, we designed the stainless steel intergranular corrosion test and stress corrosion test.

#### *3.3.1 Study on the sensitivity of the intergranular corrosion of austenitic steel*

After the chemical cleaning process, the following images were obtained from the metallographic SS304 samples of some metal test pieces. Under the 500-fold magnification of the metallographic microscope shown in Fig. 4a, no obvious intergranular corrosion was observed, which indicated that the selected cleaning process avoided intergranular corrosion. Even when  $300 \text{ mg/L Fe}^{3+}$  was added as the oxidant, the surface exhibited only mechanical treatment scratches without any traces of intergranular corrosion, as shown in Fig. 4b. This result indicated that the selected chemical cleaning solution does not cause intergranular corrosion in austenitic stainless steel during the chemical cleaning process.

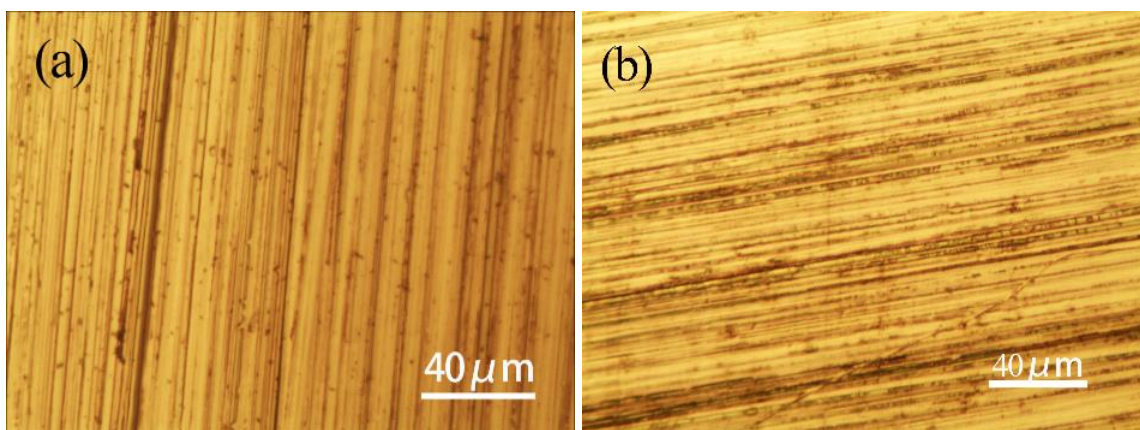


**Figure 4.** Metallographic photographs of SS304 after cleaning in glycolic acid and formic acid solution (95°C) for 48 h. (a) No  $\text{Fe}^{3+}$ ; (b) 300 mg/L  $\text{Fe}^{3+}$  added.

### 3.3.2 Study on the Stress Corrosion Sensitivity of 304 Stainless Steel

To test the impact of chemical cleaning on the austenitic stainless steel, a stress corrosion test of SS304 in glycolic acid and formic acid solution was performed. No stress corrosion cracking was observed after immersion in the cleaning solution for 120 h. Next, to increase the stress corrosion, an additional 100 mg/L of  $\text{Cl}^-$  was added to the cleaning medium, and no stress corrosion cracking was observed after 120 h.

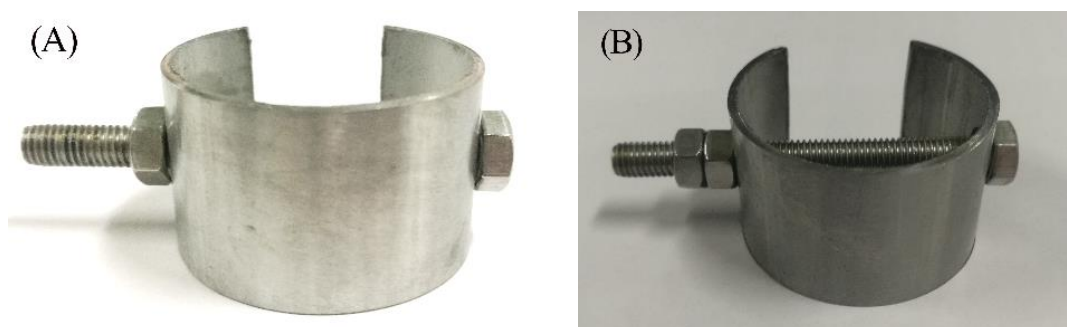


**Figure 5.** Photographs of stress corrosion of stress-loaded SS304 C-ring samples immersed in glycolic acid and formic acid solution (95°C) for 120 h. (A) Without  $\text{Cl}^-$ ; (B) with 100 mg/L  $\text{Cl}^-$  added.

In summary, the various materials subjected to the four selected cleaning processes had very low corrosion rates, which were much lower than the specified value. The selected cleaning process does not cause intergranular corrosion of austenitic stainless steel. Stress corrosion cracking does not occur for austenitic stainless steels loaded to the ultimate stress. The mechanical properties are not affected. These processes can meet the requirements of chemical cleaning of superheaters in power plants.

#### 4. DISCUSSION

In the process of chemical cleaning and dissolution of iron oxides, the electrochemical reactions that occur are mainly divided into three steps[18]. The first step is the acid-base reaction between the alkaline oxide ( $\text{Fe}_3\text{O}_4$ ) and the acidic cleaning medium, that is, the dissolution process of the oxide; see equation (1). This process is closely related to the dissolution performance of the cleaning medium and the dissolution and diffusion rate of iron oxides. Therefore, in the superheater scale cleaning process, the purpose of measures such as increasing the concentration of the cleaning medium, increasing the temperature and increasing the cleaning flow rate is to improve the reaction speed of formula (1) to improve cleaning efficiency and reduce the cleaning time. However, the corrosion rate of the metal must also be controlled, so parameters such as the moderate concentration, cleaning temperature, and flow rate usually need to be determined by corrosion tests. The second step is the electron corrosion reaction the metallic iron of the substrate; see equation (2). The usual cleaning and corrosion tests are evaluated by using metal corrosion indicators, the surface of which are polished. The difficulty of gaining and losing electrons determines the corrosion rate of metals. The third step is the reduction reaction in which electrons are gained by the ferric ions in the solution or oxide layer; see equation (3). In the chemical cleaning process, the method of adding a reducing agent is usually used to reduce the ferric iron ions in the solution to avoid the corrosion reaction between the electrons and the metal matrix.



Based on these three ion reaction equations and the corrosion phenomenon reproduced by the test of the superheater scale cleaning, the corrosion model of the scale peeling site shown in Figure 6 was established[19-21]. The process of dissolving the iron oxides and reducing the ferric ions obtained from the trivalent iron mainly occurs at the interface between the scale and the cleaning medium, and the reaction of the metal matrix losing electrons and corroding mainly occurs at the scale peeling site. Due to the high electrical conductivity of the cleaning medium, the electrochemical reaction of the two-step electron gain and loss can occur at any location between the solution and the substrate interface. During the process of oxide scale dissolution, the trivalent iron obtains electrons, and a 'large cathode' is formed. When the scale is partially exfoliated and the metal substrate is exposed to the cleaning medium, the exposed parts of the metal experience localized electron loss and corrosion. These 'large cathode' and 'small anode' battery corrosion effects accelerate the corrosion of the exposed metal at the scale peeling site, and the corrosion rate cannot be evaluated by the corrosion indicator hanging in the solution. Therefore, in the chemical cleaning of the superheater, the corrosion rate of the hanging corrosion indicator is within the range specified by the standard, but local severe corrosion thinning can still occur.

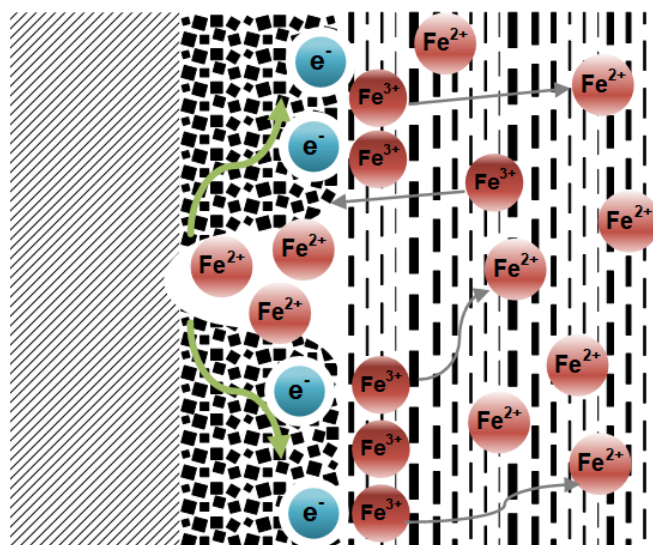


**Figure 6.** Corrosion model of the scale peeling during the cleaning process.

Due to the relatively low chromium content of metals such as 12Cr1MoV, there is no obvious iron-chromium spinel oxide layer in the oxide layer. In the later period of the cleaning of the scale, as the scale dissolves, a large amount of metal matrix is exposed to the cleaning solution. The area of the corrosion-dissolved metal ‘anode’ gradually increases, and the battery corrosion effect of the ‘large cathode’ and ‘small anode’ becomes increasingly weaker. However, the chromium content of the T91 metal is relatively high[22], and the scale is a plate-like structure. The chromium content of the oxide from the surface to the bottom gradually increases, the iron-chromium spinel oxide in the underlying oxide layer can still be intact in the later period of cleaning and remain on the surface of the metal, and the ‘small anode’ exposing the metal base does not change during the entire cleaning process. The ‘large cathode’ and ‘small anode’ occur on the metal surface in this type of superheater scale cleaning. The battery corrosion effect persists, and the corrosion is more serious than that of 12Cr1MoV.

Therefore, in the chemical cleaning of the superheater, consideration should be given to controlling the corrosion damage to the metal substrate caused by "large cathode" and "small anode" battery corrosion effects[23]. On the one hand, the cleaning formula of rapid peeling of the oxide scale can be used to shorten the exposure time of the large-area metal substrate in the cleaning solution to shorten the time of the battery corrosion effect of the "large cathode" and "small anode" and reduce the degree of local corrosion. On the other hand, a cleaning formula that uniformly distributes the redox reaction charge migration of metal corrosion across the entire cleaning interface can be used to eliminate local electron failure between the cleaning solution and the metal and oxide interface, thereby avoiding the "large cathode", and the corrosion effect of the "small anode" battery occurs during the cleaning of the oxide scale.

## 5. CONCLUSIONS

In this research, the corrosion behaviour of 12CrMoV, T91, TP310 and SS304 steels, which are widely used in boiler tubes, was studied in depth under different chemical cleaning solutions. The results from the weight-loss methods were in line with the national standards. Some solutions were highly

corrosive to carbon steel, such as 12CrMoV, and more attention should be paid to the corrosion during the project process. In addition, through the 'C-ring' test, the stress corrosion sensitivity of these steels was determined during the cleaning process. Our research on the corrosion behaviour of typical steels in chemical cleaning solutions can provide suggestions for power plant operation.

In addition to considering the above metal corrosion behaviour, the following engineering and technical difficulties should be considered in the superheater chemical cleaning of ultra-supercritical units: (1) The selection of chemical cleaning media[24]. The cleaning of the superheater needs to be considered from the two aspects of the descaling effect and the scale peeling amount to select a suitable cleaning medium. The cleaning medium should be able to fully dissolve the peeled oxide scale to avoid blockage of the pipeline. Additionally, the cleaning medium should not produce intergranular corrosion on the surface of the material, because this affects the mechanical properties of the material. (2) The accumulation of gas plugs and corrosion products should be prevented in vertical pipelines[25]. The superheater tubes are vertically arranged in a "U" or "W" shape in the furnace, with a large height difference, a compact tube bundle layout, and many elbows. Gas elbows or cleaning sediments easily create blockages at the elbows. Therefore, when chemical cleaning is performed on the superheater and reheater, it is necessary to ensure a sufficiently large flushing flux; usually, the flushing flow rate should not be less than 0.5 m/s.

## References

1. K. Abouswa, F. Elshawesh and A. Abuargoub, *Desalination.*, 222 (2008) 682.
2. W. Huang, Y. Q. Li, W. L. Xiong, S. Y. Wang, B. Feng and J. M. He, *Electric Power Construction*, 29 (2008) 94.
3. Y. Li, Z. Gao and J. M. Hou, *Thermal Power Generation*, 36 (2007) 77.
4. L. D. Zeng, K. L. Zhang, Q. J. Chen and J. M. Jia, *Electric Power*, 43 (2010) 46.
5. D. Z. Wang and X. L. Xu, *Electrical Equipment*, 9 (2008) 45.
6. J. W. Zhang, Y. M. Yuan and W. H. Liao, *Thermal Power Generation*, 39 (2010) 85.
7. X. J. Zhang, Y. Q. Deng, P. Yin and F. Liu, *Thermal Power Generation*, 43 (2014) 80.
8. W. L. Lin, Y. Q. Deng, X. J. Zhang, F. Song, L. Feng, D. D. Qi and R. T. Ni, *Corrosion & Protection*, 35 (2014) 74.
9. L. H. Zhu and D. Q. Zhang, *Cleaning World*, 31 (2015) 19.
10. C. D. Geng and H. B. Li, *Ningbo Chemical Industry*, 01 (2019) 26.
11. O. Sotelo-Mazón, C. Cuevas-Arteaga, J. Porcayo-Calderón, Rosa Ma. Melgoza-Alemán, M. G. Valladares Cisneros, G. Izquierdo-Montalvo and L. Martínez Gómez, *Int. J. Electrochem. Sci.*, 10 (2015) 9112.
12. P. Jiang, M. Dong, H. Zeng and H. J. Liu. *Power Generation Equipment*, 33 (2019) 119.
13. H. Luo and M. Gong, *Corrosion Science and Protection Technology*, 18 (2006) 357.
14. J. Y. Zhang, *Equipment Manufacturing Technology*, 2 (2012) 154.
15. Z. M. Lu, K. L. He, P. D. Huo, K. Wang and G. F. Jin, *J. Zhejiang University of Technology*, 45 (2017) 270.
16. G. Pantazopoulos, A. Vazdirvanidis and G. Tsinopoulos, *Eng. Fail. Anal.*, 18 (2011) 649.
17. C. Chen, W. J. Zhuang, X. J. Zhang and J. Y. Hu, *Thermal Power Generation*, 42 (2013) 67.
18. G. Li, L. Wang, H. Wu, C. Liu, X. Wang and Z. Cui, *Corros. Sci.*, 174 (2020) 108815.
19. M.Z. Hamzah, W.H. Yeo, A.T. Fry, J.I. Inayat-Hussain, S. Ramesh and J. Purbolaksono, *Eng. Fail. Anal.*, 35 (2013) 380.

20. P. Marek and W. Waclaw, *Eng. Fail. Anal.*, 19 (2012) 1.
21. P. Viklund, A. Hjörnhede, P. Henderson. Stålenheim and R. Pettersson, *Fuel Process. Technol.*, 105 (2013) 106.
22. X. Zhong, X. Wu and E.-H. Han, *J. Supercrit. Fluids*, 72 (2012) 68.
23. K.S.N. Vikrant, G.V. Ramareddy, A.H.V. Pavan and K. Singh, *Int. J. Pressure Vessels Piping*, 104 (2013) 69.
24. Y. Tian, *Surf. Technol.*, 05 (2016) 020.
25. J. Purbolaksono, A. Khinani, A.Z. Rashid, A.A. Ali and N.F. Nordin, *Corros. Sci.*, 51 (2009) 1022.

© 2020 The Authors. Published by ESG ([www.electrochemsci.org](http://www.electrochemsci.org)). This article is an open access article distributed under the terms and conditions of the Creative Commons Attribution license (<http://creativecommons.org/licenses/by/4.0/>).